

Assessing the dust selection bias in quasar absorbers at $0.7 < z < 1.6$: Zn/Fe abundances in a radio-selected sample.[★]

Sara L. Ellison¹ & Sebastian Lopez².

¹*Department of Physics and Astronomy, University of Victoria, Victoria, B.C., V8P 1A1, Canada*

²*Departamento de Astronomía, Universidad de Chile, Casilla 36-D, Santiago, Chile*

8 November 2018

ABSTRACT

The Complete Optical and Radio Absorption Line System (CORALS) survey has previously been used to demonstrate that the number density, gas and metals content of $z > 1.6$ damped Lyman alpha systems is not significantly under-estimated in magnitude limited surveys. In this paper, a sample of strong Mg II absorbers selected from the optically complete $0.7 < z < 1.6$ CORALS sample of Ellison et al. is used to assess the potential of dust bias at intermediate redshifts. From echelle spectra of all CORALS absorbers with Mg II λ 2796 and Fe II λ 2600 rest equivalent widths $> 0.5 \text{ \AA}$ in the redshift range $0.7 < z < 1.6$, we determine column densities of Zn, Cr, Fe, Mn and Si. The range of dust-to-metals ratios and inferred number density of DLAs from the D -index are consistent with optical samples. We also report the discovery of 4 new absorbers in the echelle data in the redshift range $1.7 < z < 2.0$, two of which are confirmed DLAs and one is a sub-DLA, whilst the Ly α line is not covered for the fourth.

Key words: quasars: absorption lines, galaxies: high redshift

1 INTRODUCTION

Galaxies contain dust. Galaxies detected through their absorption signature imprinted onto QSO spectra are no exception. The presence of dust in damped Lyman alpha (DLA) systems and other high column density absorbers has been demonstrated ubiquitously through depletion patterns of chemical elements (see the review by Wolfe et al. 2005) and more occasionally through the direct detection of some extinction feature, such as the 2175 \AA bump (Junkkarinen et al. 2004; Wang et al 2004; Ellison et al. 2006). In one case, the 9.7 μm silicate feature has been detected (Kukarni et al. 2007). Indirectly, the presence of dust can be inferred through the ratios of refractory and non-refractory elements to infer a gas-to-dust ratio, detection of molecular absorption (e.g. Noterdaeme et al. 2008), abundance ratio gradients in a DLA towards a lensed QSO (Lopez et al. 2005) and diffuse interstellar bands (York et al. 2006; Ellison et al. 2008; Lawton et al. 2008). It is therefore perhaps unsurprising that for as long as quasar absorption lines have been used to probe high redshift galaxies (e.g. Wolfe et al. 1986), there have been concerns that dust biases the results (e.g. Ostriker & Heisler 1984). Early work indicated that a significant fraction of absorption-selected galaxies might indeed be missed from surveys based on magnitude-limited optical QSO samples (Fall, Pei & McMahon 1989; Pei, Fall & Bechtold 1991; Fall & Pei 1993). More recent observations have tackled this problem with either

very large samples (Murphy & Liske 2004; Vladilo, Prochaska & Wolfe 2008), or radio-selected QSO samples (Ellison et al. 2001; Ellison, Hall & Lira 2005; Jorgenson et al 2006). Although certain special classes of QSO absorbers have been shown to exhibit substantial reddening, such as the Ca II absorbers and very high equivalent width Mg II absorbers (Wild, Hewett & Pettini 2006; Menard et al. 2008), in general reddening in the DLA absorbers is small. Although a handful of individual reddening measurements have been obtained (e.g. Vladilo et al. 2006) and a minority have quite high inferred reddening values (e.g. Junkkarinen et al. 2004), the mean $E(B-V)$ in DLAs is low. Vladilo et al. (2008) found $E(B-V) \sim 0.005 \text{ mag}$ in a large sample of DLAs selected from the magnitude limited Sloan Digital Sky Survey. Ellison et al. (2005) measured $E(B-V) < 0.04 \text{ mag}$ in an optically complete radio sample of DLAs. It is also found that the number density and total neutral gas fraction in radio-selected samples is in good agreement with large optical samples (Jorgenson et al. 2006). The typical metallicity of radio-selected samples is also only marginally higher, by 0.2 dex, than optical samples (Akerman et al. 2005). Although the extinction models presented by Vladilo & Péroux (2005) suggest that Ω_{DLA} (the neutral gas mass fraction in DLAs) is under-estimated by at least a factor of two by optical surveys, other models have come up with much lower corrections (e.g. Trenti & Stiavelli 2006). Most recently, Pontzen & Pettini (2008) have used Bayesian statistics to estimate that only 7% of DLAs are missed from magnitude limited DLA surveys with an under-estimate of Ω_{DLA} of 13%. They suggest that the larger corrections found by Vladilo & Péroux (2005) may be in part due to their smaller sample of purely optically se-

[★] Based on observations made with ESO Telescopes at the Paranal Observatories under programmes 075.A-0158 and 076.A-0389.

lected absorbers with measured abundances (that are often biased by observers' preferential selection of high $N(\text{H I})$ systems).

Although this substantial body of contemporary work has shown that there is no convincing evidence for a substantial dust bias, these results are largely limited to high redshifts, $z_{\text{abs}} > 1.5$. However, intermediate and low mass galaxies ($\log M_{\star} \lesssim 10.5 M_{\odot}$) are still actively assembling their stellar mass at this epoch with significant chemical enrichment occurring at lower redshifts (e.g. Perez-Gonzalez et al. 2008; Panter et al. 2008). Whilst one might reasonably expect the chemical evolution of the general galaxy population to evolve monotonically with redshift, the reddening and extinction of background quasars is a function of the QSO and absorber redshift, plus the extinction curve. For example, in a previous CORALS paper by Ellison, Hall & Lira (2005), the goal was to search for a reddening signature, so that the extinction curves and redshifts were accounted for in Monte Carlo simulations. In the current paper, the chemical abundances are used as an indicator of whether magnitude limited samples, on average, have distinct abundance properties compared to optically complete surveys. Given the smaller apertures of the space telescopes required to confirm low redshift DLAs, quantifying the impact on chemical abundances due to dust bias at $z < 1.5$ is particularly germane. The only assessment of the impact of dust bias at low redshifts was performed by Ellison et al. (2004). Using an optically complete radio-selected sample of quasars, Ellison et al. (2004) determined that the number density of high equivalent width (EW) Mg II absorbers was in good agreement with optical samples. 30–50% of these strong Mg II absorbers are expected to be DLAs (Rao & Turnshek 2000; Rao, Turnshek & Nestor 2006), confirmation which requires UV observations of the Ly α line. In the absence of such data (and pending the installation of a UV spectrograph on the Hubble Space Telescope, HST, during the next servicing mission), we can nonetheless assess the dust depletion in the Mg II selected absorbers of Ellison et al. (2004).

In this paper, we present the results of new observations of 16 Mg II -selected absorbers from the optically complete sample of Ellison et al. (2004). The new data consist of spectra of 15 QSOs obtained with the UV and Visual Echelle Spectrograph (UVES) on the Very Large Telescope (VLT), plus one archival spectrum obtained with the High Resolution Echelle Spectrograph (HIRES) on Keck. By comparing the ratios of Zn and Fe column densities with observations from the literature, it is shown that the dust depletion of these absorbers is commensurate with optical samples.

2 SAMPLE SELECTION

In order to assess the effect of dust bias on absorption system identification at $z < 1.7$, Ellison et al. (2004) searched for Mg II absorbers in an optically complete sample of radio-loud QSOs. Based on the observation by Rao & Turnshek (2000) and Rao et al. (2006) that absorbers with both high EWs of Fe II and Mg II have a high chance of being DLAs, we selected all absorbers in the Ellison et al. (2004) sample with $\text{EW}(\text{Fe II } \lambda 2600) > 0.5 \text{ \AA}$ and $\text{EW}(\text{Mg II } \lambda 2796) > 0.5 \text{ \AA}$ for high resolution follow-up. There are 12 such absorbers that fulfill these criteria (see Table 3 of Ellison et al. 2004)¹. In addition, there are four more absorbers with $\text{EW}(\text{Mg II } \lambda 2796) > 0.5 \text{ \AA}$

but either no coverage of Fe II $\lambda 2600$, or with an upper limit that is greater than 0.5 \AA reported in Ellison et al. (2004). In order to obtain a cleanly selected statistical sample, UVES spectra were also obtained for these four sightlines. Two of these four are found to have $\text{EW}(\text{Fe II } \lambda 2600) > 0.5 \text{ \AA}$ from our UVES spectra. In Table 1 we list the 16 absorbers, their redshifts² and Fe II and Mg II EWs as measured from the original low resolution spectra (i.e. reproduced from Table 3 of Ellison et al. 2004) or from the new UVES data (marked with a *). Since Rao et al. (2006) found that no DLA in their large (statistical) sample of 197 Mg II systems at $z < 1.65$ has an $\text{EW}(\text{Mg II } \lambda 2796) < 0.6 \text{ \AA}$, our echelle observations should include all possible DLAs from the low redshift CORALS sample.

3 OBSERVATIONS AND DATA REDUCTION

B0458–020 was observed with HIRES in February 1995 and the reduced spectrum, covering a wavelength range of 3900–6300 \AA was provided to us by J. X. Prochaska. All other data have been newly acquired with the UVES spectrograph on the VLT during ESO observing Periods 75 and 76 (April 2005 – March 2006). In all cases we used the 390+564 setting which gave wavelength coverage from approximately 3300–4500 \AA and 4600–6650 \AA . The exception to this was B1402–012 which was observed with the 437–760 setting, giving coverage from 3750–5000 \AA and 5700–9450 \AA . In Table 1 we list the exposure times for all UVES and HIRES observations. The UVES spectra were extracted and reduced using the UVES pipeline. The reduced extractions of each exposure were converted to a common vacuum-heliocentric scale, and then stacked weighting by the inverse of the flux variances.

4 COLUMN DENSITIES AND RELATIVE ABUNDANCES

The average spectral S/N ratio of our sample is lower than is typically obtained for abundance determinations. This is a result of the fact that an optically complete sample, such as CORALS from which these targets are drawn, will include many fainter QSOs than a magnitude limited sample. The lower S/N ratios hamper detailed Voigt profile decomposition, so that we instead determine total column densities using the apparent optical depth method (AODM, e.g. Savage & Sembach 1991). This technique is a widely used alternative to Voigt fitting of QSO absorption lines (e.g. Prochaska et al. 2001). Although the AODM is potentially susceptible to ‘hidden saturation’ DLA column densities derived with this method generally give good agreement with other techniques. Although Fox, Savage & Wakker (2005) showed that the AODM may overestimate column densities by $\sim 10\%$ in low S/N data, the relative abundances derived here should be unaffected by systematic offsets. We derive column densities (or limits) for Fe II, Zn II, Cr II and Mn II in the majority of our absorbers. Si II can be determined for only a small number of systems due to the low redshift range of the absorbers. When more than one transition is observed for a given species (as is often the case for Fe II), we compare the column densities derived from each to test for possible saturation (i.e. the highest f -value line yields a column density which is significantly

¹ From subsequent observations, we found that the high EW absorbers towards B0606–223 were not real. Also, the $z_{\text{abs}} = 0.7472$ absorber towards B1230–101 is now known to be a superposition of many C IV lines. The absorbers in these two lines of sight are therefore not included in our statistics.

² The absorption redshifts given in Table 1 are the original values reported by Ellison et al. (2004) for ease of reference with that work. In Table 2 we give improved redshifts derived from the new UVES data.

Table 1. Target List and Observing Journal

QSO	B mag	z_{em}	z_{abs}	EW(Mg II λ 2796) (Å)	EW(Fe II λ 2600) (Å)	Integration Time (s)	S/N pix ⁻¹ at Zn II λ 2026	Observing Period
B0039–407	19.7	2.478	0.8483	2.35 ± 0.15	2.09 ± 0.22	16,500	7	P75
B0122–005	18.5	2.280	0.9949	1.56 ± 2.08	0.56 ± 0.38	13,200	35	P75
B0227–369	19.6	2.115	1.0289	0.59 ± 0.18	0.61 ± 0.16	12,800	7	P76
B0240–060	18.7	1.805	0.5810	1.44 ± 0.08	0.69 ± 0.05*	6000	...	P76
			0.7550	1.65 ± 0.04	1.25 ± 0.04		7	
B0244–128	18.4	2.201	0.8282	1.77 ± 0.09	1.23 ± 0.09	6000	26	P76
B0458–020	19.0	2.286	1.5606	0.94 ± 0.08	0.75 ± 0.08	28,800	25	Feb 1995
B0919–260	19.0	2.300	0.7048	0.81 ± 0.08	< 0.36*	13,200	9	P75
B1005–333	18.0	1.837	1.3734	0.93 ± 0.10	0.84 ± 0.11	6600	8	P75
B1256–177	21.4	2.263	0.9399	2.96 ± 0.04	2.08 ± 0.04	13,200	7	P75
B1318–263	21.3	2.027	1.1080	1.38 ± 0.08	0.61 ± 0.07	23,100	3	P75
B1324–047	19.8	1.882	0.7850	2.58 ± 0.12	1.77 ± 0.11	19,800	7	P75
B1402–012	18.0	2.518	0.8901	1.21 ± 0.04	0.99 ± 0.04	5300	10	P75
B1412–096	17.4	2.001	1.3464	0.66 ± 0.11	0.26±0.2*	3300	10	P75
B2149–307	18.4	2.345	1.0904	1.45 ± 0.04	0.78 ± 0.04	5200	23	P75
B2245–128	18.3	1.892	0.5869	1.28 ± 0.08	0.51±0.03*	5200	...	P75

Notes: Magnitudes taken from Ellison et al. (2004). Equivalent widths are from the original low resolution data, except where marked with an asterisk (*) where they are measured from the UVES spectra. Absorbers with EW(Fe II λ 2600) < 0.5 Å are excluded from the statistical sample.

lower than the other transitions). A line that is suspected to be saturated is discarded (this process is in addition to the rejection of lines that are clearly saturated with zero residual flux in their line cores). In the absence of suspected saturation, the average of the column densities from multiple transitions is adopted. Absorption line profiles of selected transitions for our QSO sample are shown in Figures A1 – A16. We use the atomic data tabulated by Morton (2003) which is reproduced in Table B1 for ease of reference. The measured column densities are given in Table 2, as well as improved absorption redshifts derived from the UVES data. We adopt the usual assumption that the singly ionized species studied here approximate the total column density of a given element. Although there are likely to be ionization corrections for the lower $N(\text{H I})$ absorbers, we do not have the necessary data to estimate these corrections. Dessauges-Zavadsky (2003) have previously estimated that ionization corrections are likely to be on the order of 0.1 – 0.2 dex. However, such corrections are sensitive to the input ionizing spectrum and so the corrections could be significantly larger (Howk & Sembach 1999; Meiring et al. 2007). Corrections for zinc are further complicated by large uncertainties in the atomic data (Howk & Sembach 1999; Dessauges-Zavadsky et al. 2003). Although ionization corrections may therefore lead to errors in our derived column densities, this same problem should be present in the comparison data taken from the literature (at a given $N(\text{H I})$). A differential comparison between the abundance ratios in the CORALS absorbers and the optical samples taken from the literature is therefore still feasible. Observed column densities are used to derive relative abundances on the solar scale (see Table 3) and are given in Table 4. For completeness, Table 4 includes the abundances of the two absorbers (towards B0919–260 and B1412–096) subsequently found to have EW(Fe II λ 2600) < 0.5 Å, although these absorbers are not included in the statistical comparisons discussed in the next section.

Table 3. Solar meteoritic abundances from Lodders (2003)

Element, X	[X/H] _⊙
Fe	-4.53
Si	-4.46
Zn	-7.37
Cr	-6.35
Mn	-6.53

Table 4. Relative Abundances on the Solar Scale

QSO	z_{abs}	[Cr/Fe]	[Zn/Fe]	[Si/Fe]	[Mn/Fe]
B0039–407	0.84885	< +0.1	< +0.2
B0122–005	0.99430	< -0.2	+0.6	...	-0.2
B0227–369	1.02900	< -0.2	< +0.7	< +0.4	< -0.1
B0240–060	0.58103	< -0.2
B0240–060	0.75468	< -0.2	< 0.3
B0244–128	0.82850	+0.1	+0.6	...	-0.1
B0458–020	1.56055	-0.01	+0.40	+0.31	...
B0919–260	0.70527	< +0.6	< +0.8	...	< +0.2
B1005–333	1.37381	< 0	+0.5	...	< -0.7
B1256–177	0.93495	< -0.2	< +0.4	< +0.0	...
B1318–263	1.10407	< +0.4	< +1.0	...	+0.2
B1324–047	0.78472	-0.3	+0.4	...	-0.2
B1402–012	0.88978	< -0.1	+0.7	...	-0.1
B1412–096	1.34652	< +1.0	< +1.2	< +0.9	< +0.6
B2149–307	1.09074	< -0.2	< +0.1	+0.6	< -0.7
B2245–128	0.58700	< -0.4

5 RESULTS

Akerman et al. (2005) used high resolution spectra of the high redshift CORALS DLA sample to demonstrate that the metallicity (as inferred from the Zn abundance) was only marginally higher (by 0.2 dex) than the literature value at $z \sim 2.5$. Combined with the observation that the [Zn/Cr] ratios were also consistent with previous magnitude limited samples, Akerman et al. (2005) concluded that, at high redshift, dust bias does not lead to a sample that is arti-

Table 2. Measured column densities and 3σ limits for the CORALS MgII absorbers

QSO	z_{abs}	Log N(Fe II)	Log N(Cr II)	Log N(Zn II)	Log N(Si II)	Log N(Mn II)
B0039–407	0.84885	>15.0	13.3±0.2	13.2±0.1
B0122–005	0.99430	14.08±0.07	<12.1	11.8±0.2	...	11.9±0.2
B0227–369	1.02900	>14.6	<12.6	12.5±0.2	15.1±0.2	12.5±0.2
B0240–060	0.58103	14.1±0.2	<11.9
B0240–060	0.75468	14.69±0.08	<12.7	<12.1
B0244–128	0.82850	15.0±0.2	13.3±0.2	12.8±0.1	...	12.9±0.2
B0458–020	1.56055	14.92±0.05	13.09±0.05	12.48±0.05	15.3±0.1	...
B0919–260	0.70527	13.61±0.07	<12.4	<11.6	...	<11.7
B1005–333	1.37381	14.6±0.2	<12.8	12.3 ± 0.3	...	<11.9
B1256–177	0.93495	>14.7	<12.7	12.3±0.2	<14.8	...
B1318–263	1.10407	14.2±0.1	<12.8	<12.4	...	12.4±0.3
B1324–047	0.78472	15.3±0.2	13.2±0.2	12.9±0.3	...	13.1±0.2
B1402–012	0.88978	14.6±0.1	<12.7	12.5±0.2	...	12.5±0.2
B1412–096	1.34652	13.5±0.2	<12.7	<11.9	<14.5	<12.1
B2149–307	1.09074	14.25±0.09	<12.2	<11.5	14.9±0.2	<11.6
B2245–128	0.58700	14.2±0.1	<11.8

Note: Limits are 3σ and assume a line width of 7 km s^{-1} .

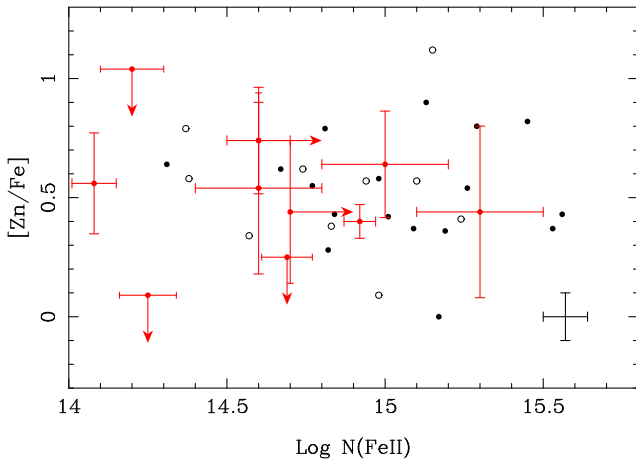


Figure 1. Comparison of $[\text{Zn}/\text{Fe}]$ as a function of $\log N(\text{Fe II})$ of literature $0.6 < z_{\text{abs}} < 1.7$ DLAs (solid black points) and sub-DLAs (open black points) with the Mg II-selected CORALS absorber (points with error bars) sample. For clarity, error bars for the literature data are not shown, but the typical error bar is shown in the lower right corner of the plot.

cially dominated by metal-poor, low dust absorbers. In the absence of neutral hydrogen column densities (only available with a space telescope), we can only use the relative abundances to investigate the possibility of dust bias. A second potential disadvantage of not having $N(\text{H I})$ is that a significant fraction of absorbers in our sample are likely to be sub-DLAs with column densities $\log N(\text{H I}) < 20.3 \text{ cm}^{-2}$. Fortunately, Dessauges-Zavadsky et al. (in preparation, see also Dessauges-Zavadsky, Ellison & Murphy 2009) have used the largest sample³ of intermediate redshift sub-DLAs yet compiled to demonstrate that the $[\text{Zn}/\text{Fe}]$ ratios in sub-DLAs are statistically indistinguishable from the DLAs. It is therefore possible to compare the $[\text{Zn}/\text{Fe}]$ relative abundances in our Mg II selected sample with a literature compilation of DLAs and sub-DLAs.

The range of Zn and Fe column densities in our sample is

commensurate with optical samples in the literature. In Figure 1 we show the relative abundances of Zn and Fe of the Mg II-selected CORALS absorbers with sub-DLAs and DLAs taken from the compilation of Dessauges-Zavadsky et al. (in preparation) whose absorption redshifts are in the range $0.6 < z_{\text{abs}} < 1.7$. If the literature sample is systematically biased against absorbers with high dust depletion, we expect that their $[\text{Zn}/\text{Fe}]$ ratios will, in general, be lower (at a given $N(\text{Fe II})$). Visually, the figure shows that the CORALS sample has $[\text{Zn}/\text{Fe}]$ ratios consistent with the literature and the two samples have identical mean values of $[\text{Zn}/\text{Fe}] = 0.55$ (detections only). This result is confirmed statistically: a 2D Kolmogorov-Smirnov (KS) test shows that there is no significant difference in the $N(\text{Fe II})$ – $[\text{Zn}/\text{Fe}]$ distribution of the CORALS and literature samples⁴. Although the samples are not selected identically (the CORALS absorbers are selected on Fe II and Mg II EWs, whilst the literature sample is selected on both on metal line EWs and $N(\text{H I})$), Figure 1 nonetheless demonstrates that the CORALS absorbers do not have particularly high dust-to-metals ratios. The one intriguing exception to this general statement is the absorber towards B1318–263. Although Zn is not detected for this system, the $[\text{Mn}/\text{Fe}]$ is super-solar by +0.2 dex, which is unusual amongst DLAs (e.g. Pettini et al. 2000; Dessauges-Zavadsky et al. 2002). Super-solar $[\text{Mn}/\text{Fe}]$ is seen in the Galactic ISM in cool disk clouds (e.g. Savage & Sembach 1996) and is usually interpreted as a signature of depletion. Only one DLA in the compilation of Dessauges-Zavadsky et al. (2002) has $[\text{Mn}/\text{Fe}] > +0.1$. The DLA towards B1318–263 may therefore be amongst the most depleted. However, even in this case the $[\text{Zn}/\text{Fe}]$ is constrained to be $< +1.0$, a value which is high amongst DLAs (see Figure 1), but still low compared to Galactic disk sightlines (e.g. Savage & Sembach 1996).

³ The sample consists of approximately 200 DLAs ($\log N(\text{H I}) \geq 20.3$) and 100 sub-DLAs ($19.0 < \log N(\text{H I}) < 20.3$) with absorption redshifts ranging from 0.01 to 4.75.

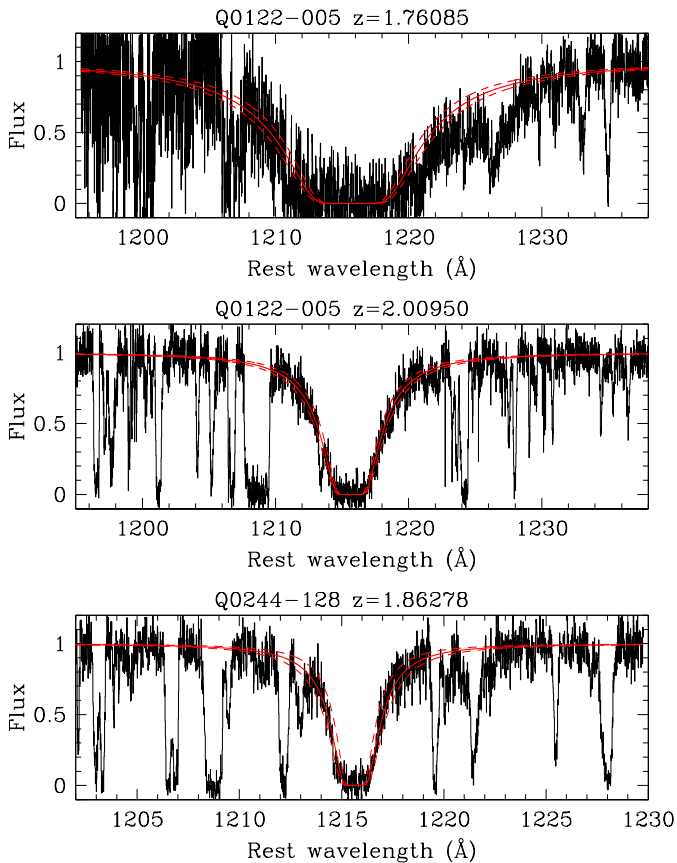


Figure 2. Fits to the Ly α profiles for the three newly discovered H I absorbers in our UVES data. Column densities and uncertainties (dashed profiles) are given in Table 5.

6 NEWLY DISCOVERED ABSORBERS IN THE UVES SPECTRA

The UVES data obtained for this study have also led to the discovery of four new absorbers which we present here for completeness. We have determined $N(\text{H I})$ column densities through fully damped Voigt-profile fits of the Ly α lines, which are shown in Figure 2. Selected metal lines of the all four absorbers are shown in Figures A17 – A20. The new absorbers consist of 1 DLA, 2 sub-DLAs and one absorber whose Ly α transition is not covered. This latter system is likely to be a DLA or high $N(\text{H I})$ sub-DLA based on its strong metal lines. The column densities were derived through the AODM method and are presented in Table 5.

7 SUMMARY AND DISCUSSION

Akerman et al. (2005) showed that the dust-to-metals ratio of CORALS DLAs was consistent with DLAs from magnitude limited literature samples. It was argued that this was evidence against a particularly dusty population of DLAs at $1.7 < z_{\text{abs}} < 3.5$. In this

paper, we have extended that conclusion down to lower redshifts, where galaxies may be more chemically evolved. We have compiled an optically complete sample of absorbers with strict selection criteria of $\text{EW}(\text{Fe II } \lambda 2600, \text{Mg II } \lambda 2796) > 0.5 \text{ \AA}$. In our sample of 14 $0.6 < z_{\text{abs}} < 1.7$ Mg II -selected absorbers fulfilling these EW criteria, we can determine values or limits for $[\text{Zn}/\text{Fe}]$ for 11 absorbers. The relative abundances are commensurate with the distribution in the literature for DLAs and sub-DLAs. This result adds to the growing body of observational evidence that, although dust is present in absorption selected galaxies, the observational bias imposed by this dust does not strongly affect the statistical properties of the DLA population.

The obvious next step from the current work is to determine $N(\text{H I})$ for the CORALS absorbers presented here. H I column density measurements would allow us to a) confirm which of the absorbers are truly DLAs, b) determine absolute abundances and c) derive spin temperatures for the subset of absorbers with 21cm observations presented in Kanekar et al. (2009). Out of the 14 Mg II absorbers in our EW-selected sample, Kanekar et al. (2009) have obtained 21 cm absorption spectra for 11. Nine absorbers have both measurements (or limits) of the Zn column density and 21 cm optical depth. Based on a dataset of 25 points over all redshifts, Kanekar et al. (in preparation) show that metallicity may be anticorrelated with spin temperature. However, since it has been suggested that the 21cm detection rate and spin temperature of DLAs may evolve with redshift (e.g. Kanekar et al. 2003; Kanekar et al. 2009), with only one known DLA at $z > 1.7$ exhibiting a spin temperature below 500 K (York et al. 2007), it would be desirable to consider the relation of spin temperature with metallicity as a function of redshift. Only 9 absorbers currently have measurements of both Zn and 21 cm optical depth at $z < 1.7$. Obtaining Ly α observations of the nine systems in the current sample with measurements of both $N(\text{Zn II})$ and $\tau_{21\text{cm}}$ would therefore double the low redshift sample in which this relation could be investigated.

H I observations (at the present time) require HST spectroscopy and are therefore pivotal to the successful installation of the Cosmic Origins Spectrograph (COS) and/or the repair/upgrade of the Space Telescope Imaging Spectrograph (STIS) scheduled for Servicing Mission 4. The design of such observations would prioritise likely DLAs over sub-DLAs in order to make the direct comparison of metallicities in magnitude limited and optically complete samples. Although the current work has shown that dust-to-gas ratios in the low redshift CORALS sample are typical, a comparison of metallicities (as done by Akerman et al. 2005 for the high redshift CORALS sample) is required in order to assess the fraction of missing metals. The high resolution spectra presented here can be used to guide those observations, by assessing which of the Mg II -selected absorbers are unlikely to be DLAs. Ellison (2006) investigated how the combination of EW and kinematic information from high resolution spectra could be used to screen for DLAs. Ellison (2006) introduced the D -index which is a measure of saturation over the velocity profile over the Mg II $\lambda 2796$ line with DLAs tending to have higher values than sub-DLAs, as measured in high resolution data. Specifically, Ellison (2006) defined

$$D = \frac{\text{EW}(\text{\AA})}{\Delta v(\text{km/s})} \times 1000, \quad (1)$$

where the EW and velocity spread of the Mg II $\lambda 2796$ line are measured over 90% of the EW of the main absorption component. In a more recent study, Ellison et al. (2008) have shown that including the Fe II column density slightly improved the discriminating power of the D -index and defined

⁴ This is true regardless of whether limits are included or whether only detections are used in the KS test.

Table 5. Measured column densities for the newly discovered absorbers in the UVES spectra

QSO	z_{abs}	$N(\text{H I}) (10^{19} \text{ cm}^{-2})$	$\text{Log } N(\text{Fe II})$	$\text{Log } N(\text{Cr II})$	$\text{Log } N(\text{Zn II})$	$\text{Log } N(\text{Si II})$
B0122–005	1.76085	60±10	15.1±0.1	13.4±0.2	...	15.42±0.08
B0122–005	2.00950	11±2	13.69±0.07	<12.1	<11.4	13.67±0.05
B0244–128	1.86278	3±1	<13.9	12.2±0.3	<11.5	14.2±0.2
B2149–307	1.70085	...	15.0±0.1	13.2±0.2	12.6±0.1	15.4±0.1

$$D_{\text{Fe}} = \frac{EW(\text{\AA})}{\Delta v(\text{km/s})} \times \frac{\log N(\text{Fe II})}{15} \times 1000 \quad (2)$$

Ellison et al. (2008) found that ~ 54 and 57% of absorbers with $D > 7.2$ and $D_{\text{Fe}} > 7.0$ respectively are DLAs.

We calculate the D-index for the absorbers in our sample using the UVES data. For B0458–020, the HIRES spectra did not cover the $\text{Mg II } \lambda 2796$ line, but a UVES spectrum was available in the archive that did possess the requisite wavelength coverage. For 2 of our absorbers (B0227–369 and B1402–012), the Mg II line lies in the UVES chip/inter-arm gaps, so the D-index could not be calculated.

In Table 6 we present the values of D_{Fe} for our Mg II sample. Again, for completeness, we include the indices for the two absorbers with $EW(\text{Fe II } \lambda) < 0.5 \text{ \AA}$, but do not consider them in our statistics. From the statistical sample of 14 absorbers, nine have $D_{\text{Fe}} > 7.0$, three have $D_{\text{Fe}} < 7.0$ and two have insufficient information to judge. The three low D -index absorbers are unlikely to be DLAs (see Figure 7 of Ellison et al. 2008). However, only five of the nine high D -index absorbers are statistically likely to be DLAs, based on the success rate of the D-index. We therefore statistically expect $5/12 = 42\%$ to actually be DLAs. This is in good agreement with the fraction of DLAs expected from Mg II and Fe II EWs alone (which formed the initial selection of the sample), $36 \pm 6\%$ as found by Rao et al. (2006). This DLA fraction can be scaled up to the full statistical sample of 14 absorbers and combined with the redshift paths in Ellison et al. (2004) to determine the number density of DLAs in the intermediate redshift CORALS sample. Using errors appropriate for small samples (Gehrels 1996), we determine $n(z) = 0.11^{+0.07}_{-0.04}$ for a mean absorption redshift of $\langle z_{\text{abs}} \rangle = 1.0^5$. It should be noted that the original intermediate redshift CORALS sample presented in Ellison et al. (2004) omitted two QSOs due to their faint magnitudes and limited observing time. The detection of an absorber with Mg II , Fe II EW $> 0.5 \text{ \AA}$ and a D -index > 7.0 in either one or both of these sightlines would increase the inferred number density to $n(z) = 0.12$ and 0.14 respectively. The $n(z)$ is therefore in excellent agreement with the value of $n(z) = 0.120 \pm 0.025$ at $\langle z_{\text{abs}} \rangle = 1.2$ derived by Rao et al. (2006) from their HST survey. Taken together with the consistency of Zn/Fe ratios between the CORALS DLAs and the literature, the concordant DLA number densities of CORALS and the HST survey (despite the relatively bright magnitude limit of the latter), im-

⁵ The derived $n(z)$ for DLAs based on the D-index is slightly lower than the value found by Ellison et al. (2004) ($n(z) = 0.16^{+0.08}_{-0.06}$) for the CORALS Mg II absorbers based on EW statistics. The main difference is due to updated results from Rao et al. (2006) regarding the likelihood that a strong Mg II absorber is a DLA, a probability that has dropped from 50% to 35% since Rao & Turnshek (2000). Moreover, Ellison et al. (2004) used 5σ significance limits, whereas we have adopted 3σ . Taking into account these two differences, the DLA $n(z)$ derived purely from EW statistics for CORALS is $0.13^{+0.07}_{-0.05}$, in good agreement with the incidence rate derived from D-index statistics.

Table 6. D-indices for the CORALS Mg II absorbers

QSO	z_{abs}	D_{Fe}
B0039–407	0.84885	≥ 8.94
B0122–005	0.99430	5.15±0.19
B0227–369	1.02900	...
B0240–060	0.58103	7.49±0.23
B0240–060	0.75468	5.43±0.43
B0244–128	0.82850	9.11±0.12
B0458–020	1.56055	6.75±3.39
B0919–260	0.70527	5.60±0.22
B1005–333	1.37381	8.74±0.58
B1256–177	0.93495	≥ 8.30
B1318–263	1.10407	7.25±0.85
B1324–047	0.78472	8.51±0.31
B1402–012	0.88978	...
B1412–096	1.34652	6.59±1.00
B2149–307	1.09074	7.91±0.25
B2245–128	0.58700	7.03±0.43

plies that optically selected samples of intermediate redshift DLAs are not missing a significant population of absorbers, and that their dust depletion properties are representative of the full population of DLAs.

ACKNOWLEDGMENTS

SLE is supported by an NSERC Discovery Grant and SL was partly supported by the Chilean *Centro de Astrofísica* FONDAF No. 15010003, and by FONDECYT grant N°1060823.. We are grateful to J. X. Prochaska for providing the HIRES spectrum of B0458–020 and to Nissim Kanekar for useful comments on an earlier draft of this paper.

REFERENCES

- Akerman, C. J., Ellison, S. L., Pettini, M., Steidel, C. C. 2005, *A&A*, 440, 499
 Dessauges-Zavadsky, M., Prochaska, J. X., & D’Odorico, S., 2002, *A&A*, 391, 801
 Dessauges-Zavadsky, M., Péroux, C., Kim, T.-S., D’Odorico, S., McMahon, R. G., 2003, *MNRAS*, 345, 447
 Dessauges-Zavadsky, M., Ellison, S. L., Murphy, M. T., 2009 *MNRAS*, accepted
 Ellison, S. L., Yan, L., Hook, I., Pettini, M., Wall, J., Shaver, P., 2001, *A&A*, 379, 393
 Ellison, S. L., Churchill, C. W., Rix, S. A., Pettini, M., 2004, *ApJ*, 615, 118
 Ellison, S. L., Hall, P. B., Lira, P., 2005, *AJ*, 130, 1345
 Ellison, S. L., 2006, *MNRAS*, 368, 335
 Ellison, S. L., et al. 2006, *MNRAS*, 372, L38
 Ellison, S. L., York, B. A., Murphy, M. T., Zych, B. J., Smith, A., Sarre, P., 2008, *MNRAS*, 383, L30

Fall, S. M., Pei, Y., 1993, *ApJ*, 402, 479
 Fall, S. M., Pei, Y., McMahon, R. G., 1989, *ApJ*, 341, L5
 Fox, A. J., Savage, B. D., & Wakker, B. P., 2005, *AJ*, 130, 2418
 Howk, J.C., & Sembach, K.R. 1999, *ApJ*, 523, L141
 Jorgenson, R., Wolfe, A. M., Prochaska, J. X., Lu, L., Howk, J. C., Cooke, J., Gawiser, E., Gelino, D., 2006, *ApJ*, 646, 730
 Junkkarinen, V. T., Cohen, R. D., Beaver, E. A., Burbidge, E. M., Lyons, R. W., Madejski, G., 2004, *ApJ*, 614, 658
 Kanekar, N., Prochaska, J. X., Ellison, S. L., Chengalur, J. N., *MNRAS*, accepted, arXiv:0903.4487
 Kulkarni, V., York, D. G., Vladilo, G., Welty, D. E., 2007, *ApJ*, 663, L81
 Lawton, B., Churchill, C., York, B., Ellison, S. L., Snow, T., Johnson, R., Ryan, S., 2008, *AJ*, 136, 994
 Lopez, S., Reimers, D., Gregg, M. D., Wisotzki, L., Wucknitz, O., Guzman, A., 2005, *ApJ*, 626, 767
 Meiring, J. D., Lauroesch, J. T., Kulkarni, V. P., Peroux, C., Khare, P., York, D. G., Crotts, A. P. S., 2007, *MNRAS*, 376, 557
 Menard, B., Nestor, D., Turnshek, D., Quider, A., Richards, G., Chelouche, D., Rao, S., 2008, *MNRAS*, 385, 1053
 Murphy, M. T., & Liske, J., 2004, *MNRAS*, 345, L31
 Noterdaeme, P., Ledoux, C., Petitjean, P., Srianand, R., 2008, *A&A*, 481, 327
 Ostriker, J. P., Heisler, J., 1984, *ApJ*, 278, 1
 Panter, B., Jimenez, R., Heavens, A. F., Charlot, S., 2008, *MNRAS*, 391, 1117
 Pei, Y., Fall, S. M., Bechtold, J., 1991, *ApJ*, 378, 6
 Perez-Gonzalez, P. G., et al., 2008, *ApJ*, 675, 234
 Pontzen, A., & Pettini, M., 2008, *MNRAS* accepted, arXiv:0810.3236v2
 Prochaska, J. X., Wolfe, A., Tytler, D., Burles, S., Cooke, J., Gawiser, E., Kirkman, E., O'Meara, J., Storrie-Lombardi, L., 2001, *ApJS*, 137, 21.
 Rao, S.M., & Turnshek, D.A. 2000, *ApJS*, 130, 1
 Rao, S.M., Turnshek, D.A., Nestor, D. B., 2006, *ApJ*, 636, 610
 Savage, B. D. & Sembach, K. R., 1991, *ApJ*, 379, 245
 Savage, B. D. & Sembach, K. R., 1996, *ARA&A*, 34, 279
 Trenti, M., & Stiavelli, M., 2006, *ApJ*, 651, 51
 Vladilo, G., & Péroux, C., 2005, *A&A*, 444, 461
 Vladilo, G., Centurion, M., Levshakov, S., Peroux, C., Khare, P., Kulkarni, V., York, D. G., 2006, *A&A*, 454, 151
 Vladilo, G., Prochaska, J. X., Wolfe, A. M., 2008, *A&A*, 478, 701
 Wang, J., Hall, P. B., Ge, J., Li, A., Schneider, D., 2004, *ApJ*, 609, 589
 Wild, V., Hewett, P. C., & Pettini, M., 2006, *MNRAS*, 367, 211
 Wolfe, A. M., Turnshek, D. A., Smith, H. E., & Cohen, R. D. 1986, *ApJS*, 61, 249
 Wolfe, A., Gawiser, E., & Prochaska, J. X., 2005, *ARA&A*, 43, 861
 York, B. A., Ellison, S. L., Lawton, B., Churchill, C. W. C., Snow, T., Johnson, R., Ryan, S., 2006, *ApJ*, 647, L29

APPENDIX A: ABSORPTION LINE FIGURES

Figures A1 – A20 show selected metal lines for all absorption systems included in this study.

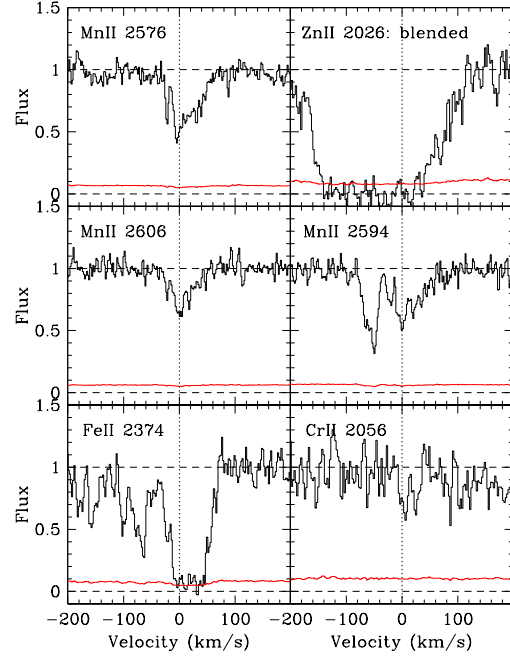


Figure A1. Metal lines towards B0039–407 on a velocity scale relative to $z = 0.84885$

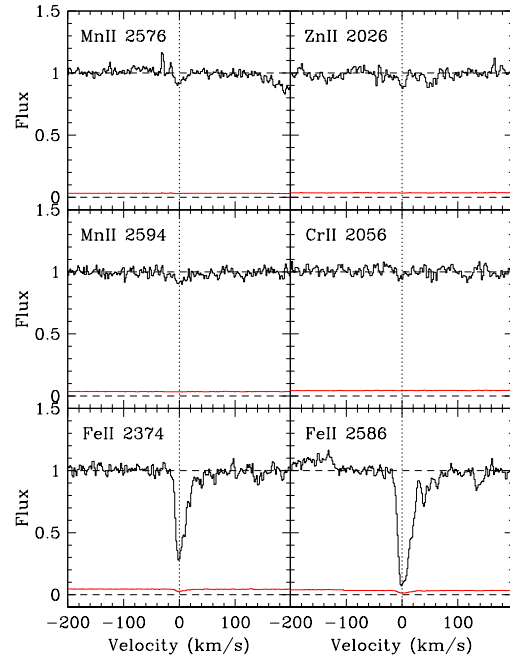


Figure A2. Metal lines towards B0122–005 on a velocity scale relative to $z = 0.99430$

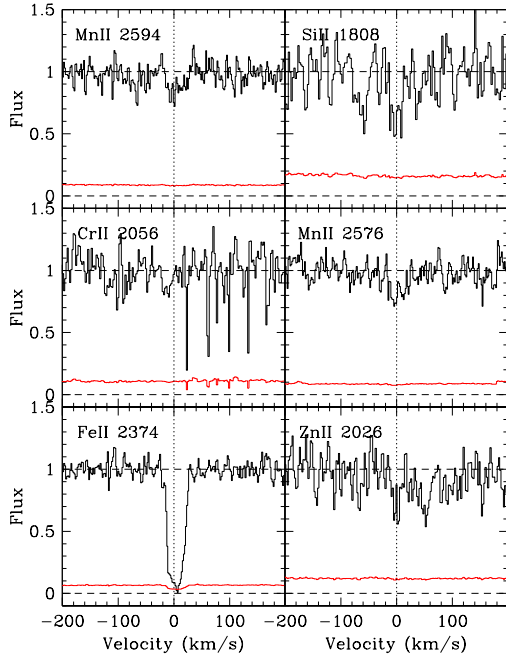


Figure A3. Metal lines towards B0227–369 on a velocity scale relative to $z = 1.02900$

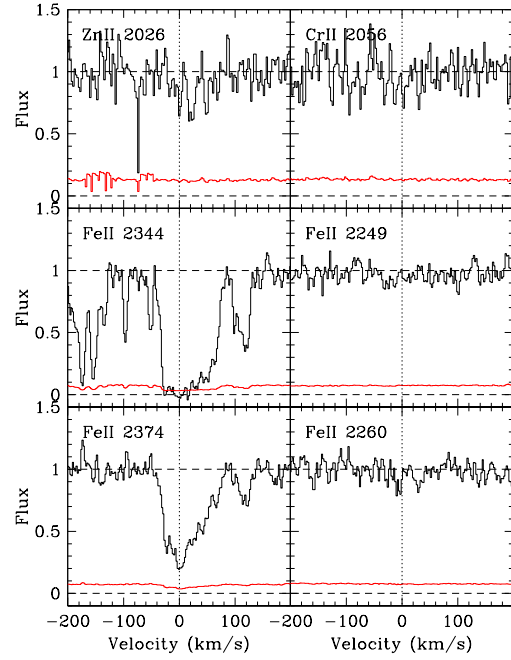


Figure A5. Metal lines towards B0240–060 on a velocity scale relative to $z = 0.75468$

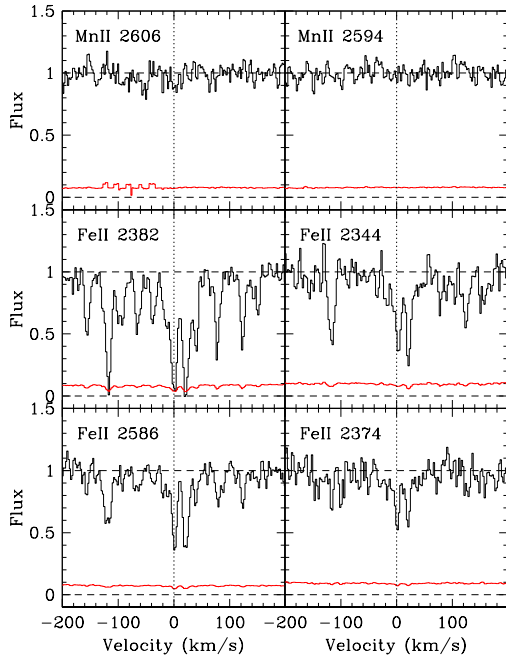


Figure A4. Metal lines towards B0240–060 on a velocity scale relative to $z = 0.58103$

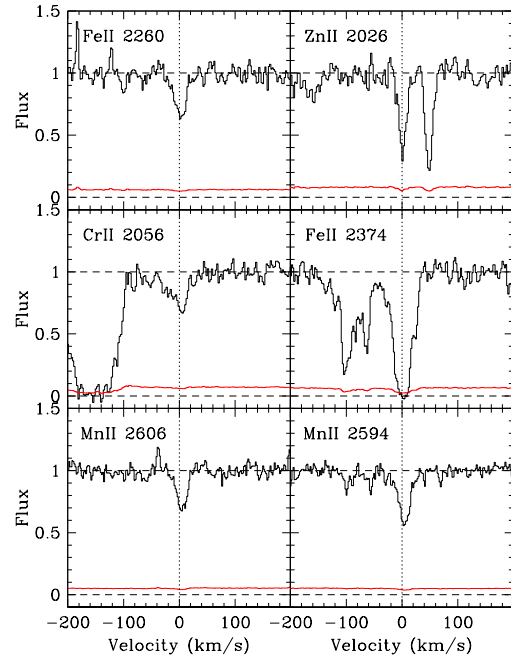


Figure A6. Metal lines towards B0244–128 on a velocity scale relative to $z = 0.82850$

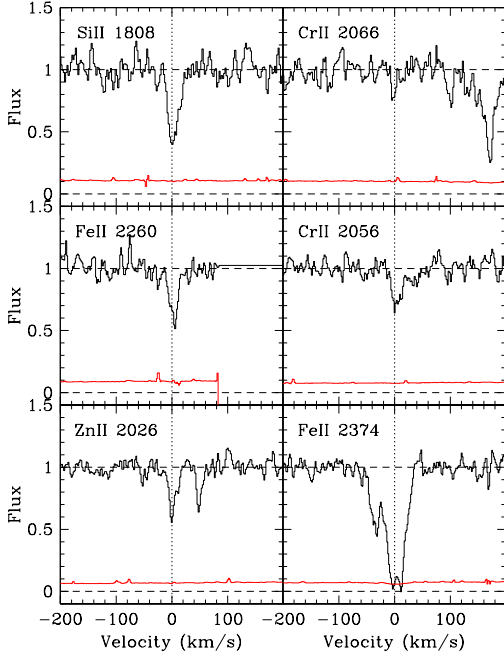


Figure A7. Metal lines towards B0458–020 on a velocity scale relative to $z = 1.56055$

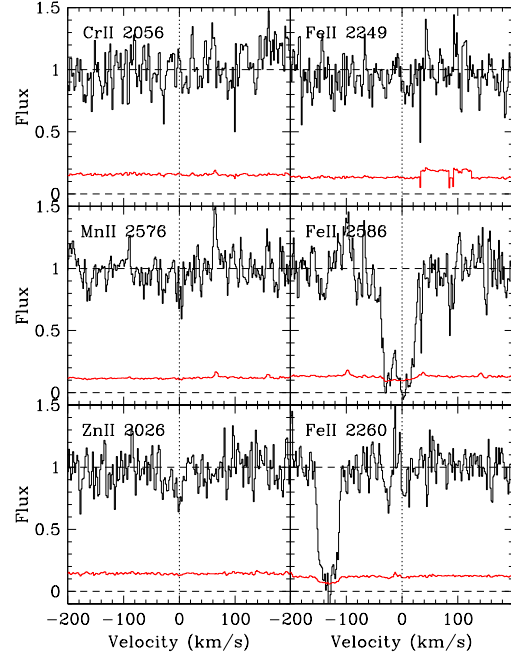


Figure A9. Metal lines towards B1005–333 on a velocity scale relative to $z = 1.37381$

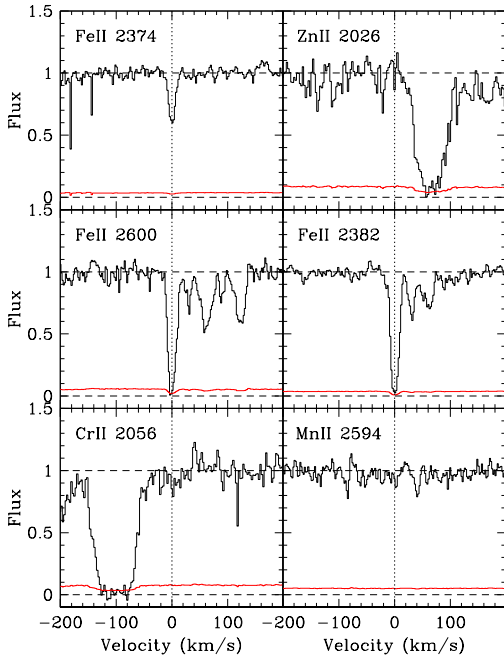


Figure A8. Metal lines towards B0919–260 on a velocity scale relative to $z = 0.70526$

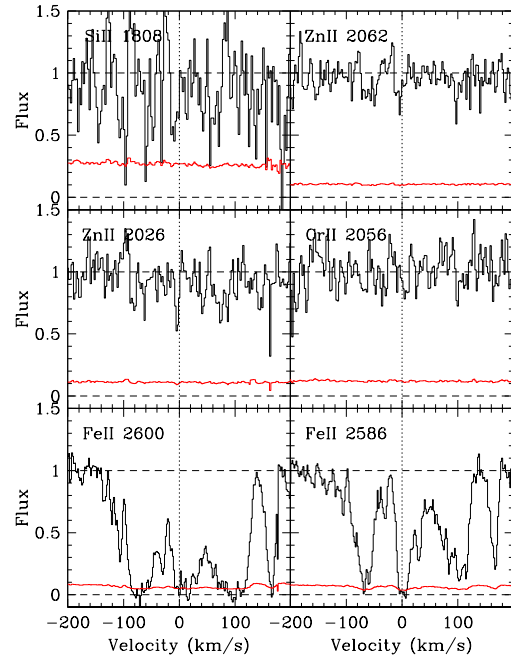


Figure A10. Metal lines towards B1256–177 on a velocity scale relative to $z = 0.93495$

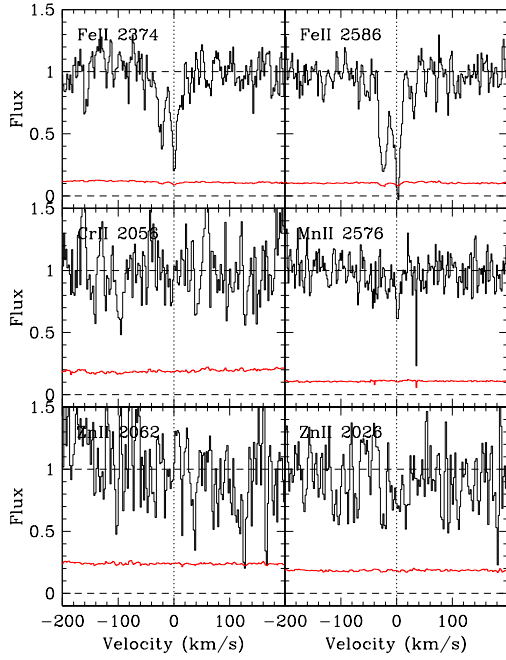


Figure A11. Metal lines towards B1318–263 on a velocity scale relative to $z = 1.10407$

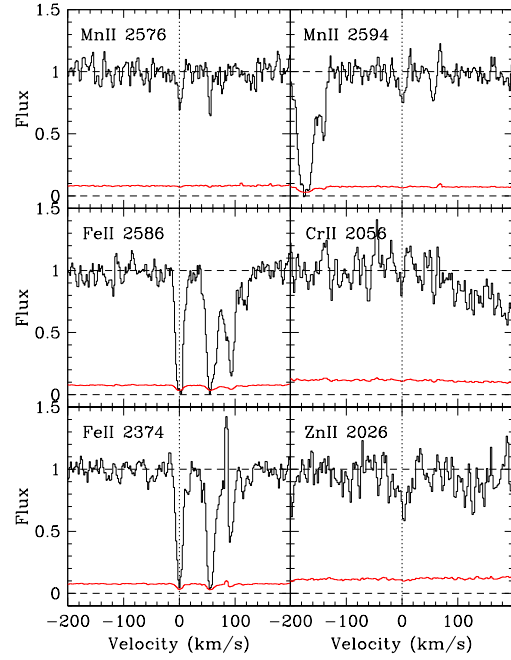


Figure A13. Metal lines towards B1402–012 on a velocity scale relative to $z = 0.88978$

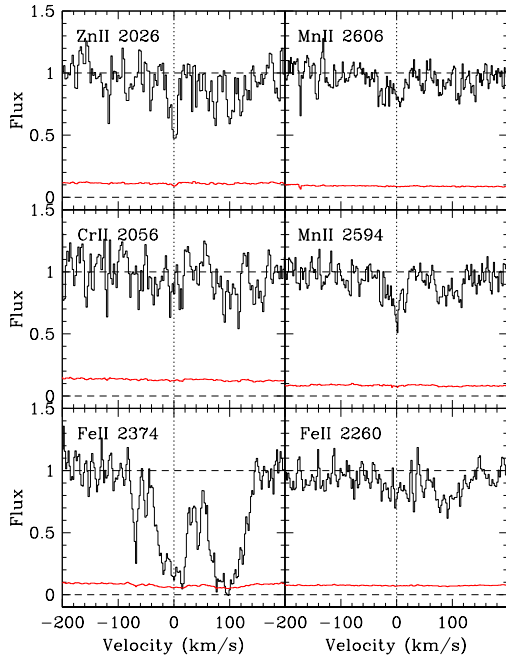


Figure A12. Metal lines towards B1324–047 on a velocity scale relative to $z = 0.78472$

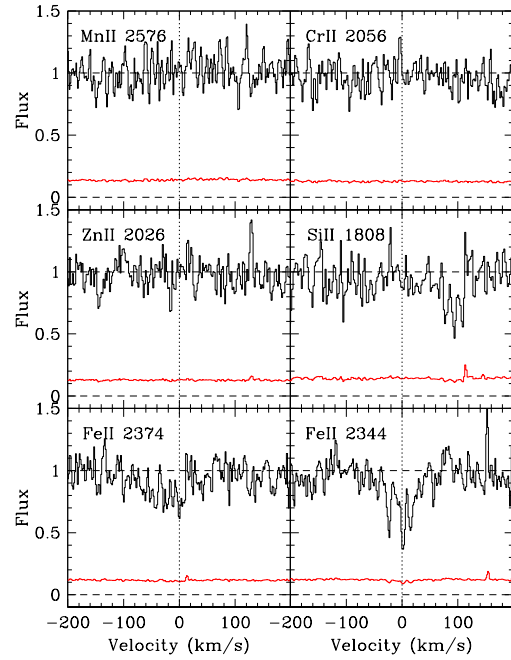


Figure A14. Metal lines towards B1412–096 on a velocity scale relative to $z = 1.34652$

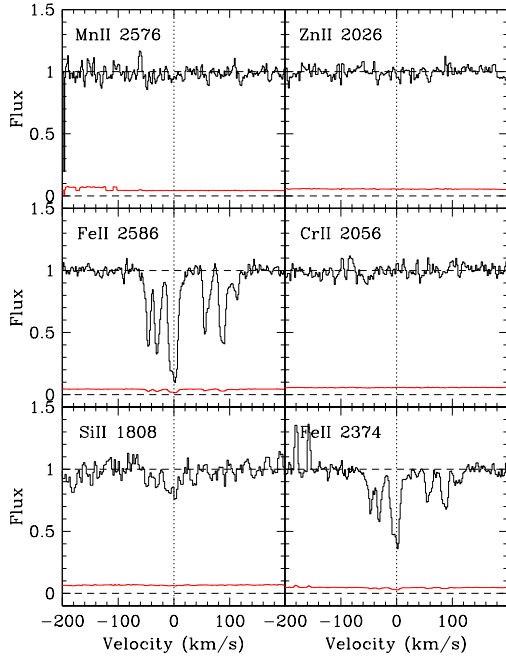


Figure A15. Metal lines towards B2149–307 on a velocity scale relative to $z = 1.09074$

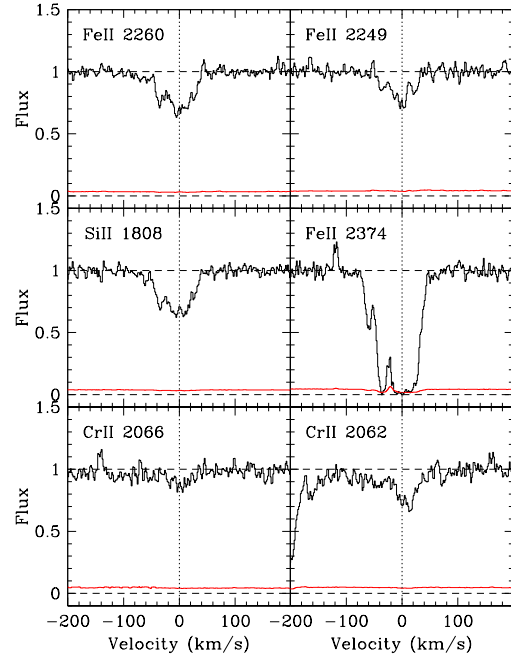


Figure A17. Metal lines towards B0122–005 on a velocity scale relative to $z = 1.76085$

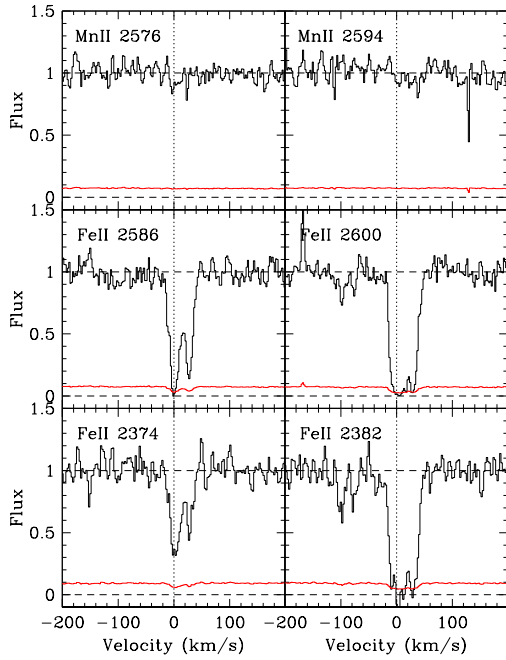


Figure A16. Metal lines towards B2245–128 on a velocity scale relative to $z = 0.58700$

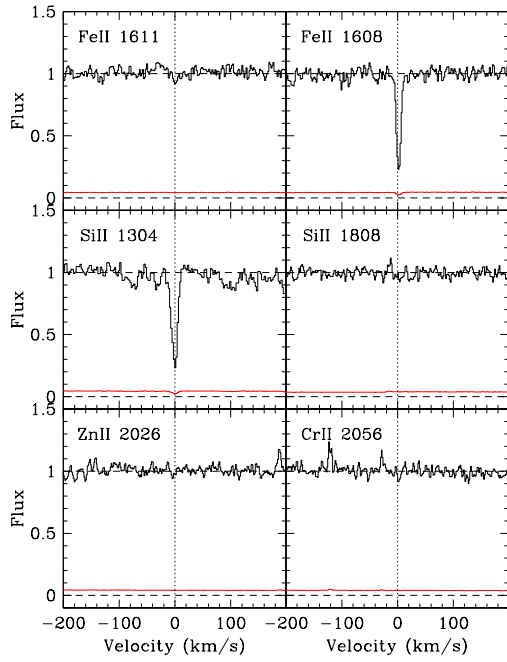


Figure A18. Metal lines towards B0122–005 on a velocity scale relative to $z = 2.00950$

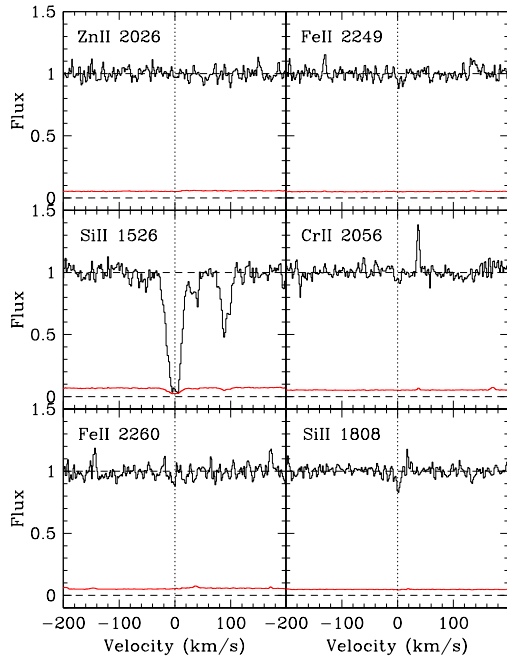


Figure A19. Metal lines towards B0244–128 on a velocity scale relative to $z = 1.86278$

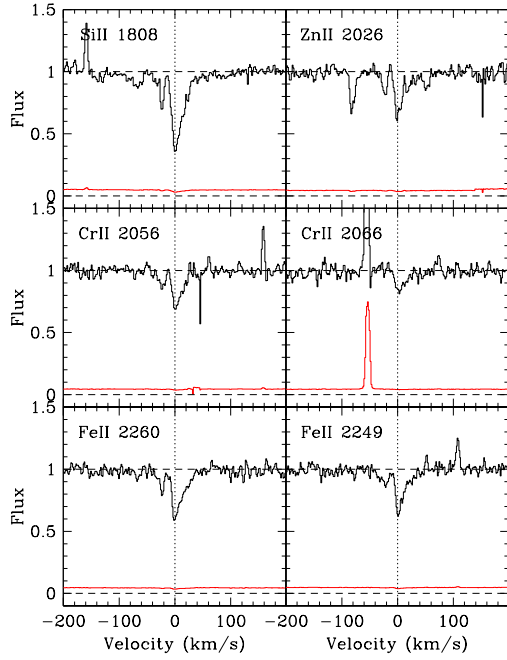


Figure A20. Metal lines towards B2149–307 on a velocity scale relative to $z = 1.70085$

Table B1. Atomic data for the detected transitions from Morton (2003)

Species	λ	f
Si II	1304.3702	0.094
Si II	1808.0130	0.002186
Cr II	2056.2539	0.10500
Cr II	2062.2340	0.07800
Cr II	2066.1610	0.05150
Fe II	2600.1729	0.2390
Fe II	2586.6500	0.06910
Fe II	2382.7650	0.3200
Fe II	2374.4612	0.0313
Fe II	2344.2140	0.1140
Fe II	2260.7805	0.00244
Fe II	2249.8768	0.001821
Fe II	1608.4511	0.05800
Zn II	2062.6640	0.2560
Zn II	2026.1360	0.4890
Mn II	2606.4620	0.1927
Mn II	2594.4990	0.2710
Mn II	2576.8770	0.3508

APPENDIX B: ATOMIC DATA

In Table B1 we reproduce the atomic data used in our column density determinations.